bioRxiv (2023)
doi:10.1101/2021.11.27.470200
a Malthusian Relativity paper

$\iota^{**}=7/3\psi$
mrLife.org

Population dynamic life history models for 9,488 bird and 4,865 mammal species

Lars Witting
Greenland Institute of Natural Resources, Box 570, DK-3900 Nuuk, Greenland. email:lawi@natur.gl

Abstract Freely accessible ready-to-use population dynamic simulations can inform conservation decisions when time and/or economy is too limited for data collection and subsequent analysis. Yet, this requires species specific models as the dynamics of each species is unique because the demography and population regulation varies among species. By estimating the age-structured demography of birds and mammals with body mass estimates, I provide a first step towards the construction of a library of population dynamic simulations for all species. Combining life history data and allometric theory, I estimate missing parameters by allometric correlations at the lowest taxonomic level. This provides complete population models for 9,488 bird and 4,865 mammal species, covering 27 life history and ecological traits per species. I use the estimates to analyse for evolutionary differences between birds, placentals, marsupials and bats, and I illustrate the next step by fits to timeseries data explaining a diverse range of population dynamic trajectories.

Keywords: Life history, demography, bird, mammal, allometry, population dynamics

1 Introduction

Climate change and biodiversity loss are major challenges imposed by the expanding demands of our growing human population. While climate change contributes, the primary cause for the loss of biodiversity is our use of land and sea. One concern is the conversion of land to agricultural and urban use, removing and fragmentating habitats required for the survival of many species.

A solution to the biodiversity crisis requires political courage, and scientist can help by integrating biological data into measures, models, and analyses that are easy to interpret and use. This applies not only where data are available, but also by extrapolating our best scientific knowledge for the use in critical cases where actions are needed but time and/or economy is too limited for data collection and subsequent analysis.

The Living Planet Index (LPI) is one example that measures the joint trend in the diversity of animal life on Earth from timeseries of abundance of almost 40,000 populations of more than 5,000 species of vertebrates from terrestrial, freshwater, and marine habitats. According to this indicator, the trend of global vertebrate abundance is a steady decline, with an average decline of about 70% from 1970 to 2018 across all monitored populations (LPI 2022). Luckily, the LPI gives a false impression because the estimated decline is imposed by outliers, with 98.6% of the vertebrate populations across all systems showing no mean global trend (Leung et al. 2020). This highlights the need for detailed analyses to understand the conservation implications of trends, identifying species and regions with need for urgent action, as well as areas that improve.

As population trends can have many causes, their population biological implications are not always as straightforward as they seem. Successful trend analyses depend on realistic population models that can identify the underlying causes from timeseries data. With this paper I initiates a project that uses population dynamic timeseries data from the LPI and other sources to estimate first-approximation population dynamic models for all species of birds and mammals with an estimate of body mass. Apart from analysing the underlying causes of existing timeseries, a main goal of the project is to construct a library of Bird and Mammal Populations (BMP, at https://mrLife.org/bmp.htm) that is freely available for online simulations. This allows for population dynamic analyses of all species, including the estimation of expected trajectories given habitats that fragment or improve.

The development of BMP includes three relatively independent stages, with this paper covering the first. Apart from externally imposed variation and trends, the population dynamics of a species is determined by its age-structured demography and population regulation by density dependent competition and density dependent natural selection. While the two regulating forces can be estimated from population dynamic timeseries, these data are generally insufficient for the estimation of the age-structure. Hence, in this first stage I use life history data to estimate complete age-

structured models for all species with an estimate of mass. Having the age-structure demography I proceed in phase two with the estimation of population regulation for all species with timeseries data of sufficiently high quality (following the approach in Witting 2021), before the estimates of regulation are extrapolated across species in phase three.

Instead of restricting my estimates of age-structure to the demographic parameters that are necessary for the population dynamic models, I use the theoretical framework of Malthusian relativity (Witting 1997, 2008, 2017a,b) to estimate much broader equilibrium life history models with zero population dynamic growth based on the energetics and ecology of each species. These models have a strong theoretical basic, and a wider range of potential uses, as illustrated in the result section by a short analysis on the evolutionary life history differences between birds, placentals, marsupials, and bats. Being based on Witting (2017a), the models balance the estimates of the different parameters in accordance with a population dynamic feed-back selection that integrates the competition-dependent consumption of energy across the interacting individuals in the population. This describes the natural selection of the life history in general (Witting 2008), including predictions of inter-specific allometric correlations (Witting 1995, 2017a).

Each of these species models integrates foraging in home ranges at the population dynamic equilibrium abundance, with a metabolism driven consumption of net energy for a reproduction that is constrained by the energetic growth of offspring and the age-structured demography, with all components being balanced against one another to produce zero population dynamic growth. As illustrated by examples at the end of the paper, I need only include two extra population regulation parameters to extend these single species models into complete population dynamic simulations.

1.1 Inter-specific extrapolations

To estimate the missing parameters of the life history models of the different species I combine large datasets published over the past couple of decades with inter-specific extrapolations by allometric correlations, based on the allometric theory of Malthusian relativity. Following this method, the minimum requirement for a species model is an estimate of body mass, with Smith et al. (2004) providing 4,361 body mass estimates for mammals, and Dunning (2007) similar estimates for more than 8,700 species of birds.

Body mass estimates are often published in allometric studied with other traits (e.g., Bonner 1965; Schoener 1968; Turner et al. 1969; Fenchel 1974; Damuth 1981, 1987; Peters 1983; Calder 1984), leading to the accumulation of basal metabolic rates for more than 700 species of mammals (McNab 2008) and 350 species of birds (McKechnie and Wolf 2004), with independent estimates of field metabolism (Hudson et al. 2013). Life history parameters on reproduction, physiological time periods, and individual growth were collected in large datasets by Jetz et al. (2008), De Magalhães and Costa (2009), Jones et al. (2009), and Myhrvold et al. (2015). Survival estimates are available from McCarthy et al. (2008), DeSante and Kaschube (2009), and Ricklefs et al. (2011), and ecological traits like population densities and home range areas were published by Damuth (1987), Tucker et al. (2014), Tamburello et al. (2015), Nasrinpour et al. (2017), and Santini et al. (2018).

To extrapolate life history models across species, I combine the diverse data into a single dataset, and use standard calculations to transform some of the data into common parameters. The data are then checked for outliers and combined with allometric calculations to estimate the missing values for all species with a data-based estimate of body mass. This generates equilibrium life history models for 89.4% of the bird species in Gill and Donsker (2014), and 89.1% of the mammals in Wilson and Reeder (2005).

2 Methods

All the estimated models are similar to the theoretical model that Witting (1995, 2017a,b) used to deduce the evolution of inter-specific allometries from the natural selection of metabolism, body mass, and the life history and population dynamic foraging ecology as a whole. For a description of the underlying population dynamic feedback selection, you will have to consult these papers, as I restrict myself to the estimation of the underlying population level parameters of the different species, including the average life histories across the individuals of a population. Some essential relations between the different traits are described in Appendix A and B, with the overall model divided into the four components of individual growth, demographic traits, life history energetics, and population ecology. In the four sub-sections below, I briefly describe all the parameters that I estimate.

2.1 Individual growth

The growth of an individual with age is described by

	w	w_0	w_j	β	$\underline{\beta}$	t_p	t_j	t_s	t_m	t_l	m_b	m_f	m_i	p_{ad}	N	h
Aves	9488	778	207	76	356	2238	1822	1211	681	1674	7045	1772	0	869	1277	221
Mammalia	4865	1869	1058	57	708	2219	2042	1999	931	2617	3512	2147	651	276	1107	441

	w	$\acute{w}_0$	$\acute{w}_j$	β	t_x	m	R	l_m	l_r	ϵ	α	N	b	ϵ_n	h	h_o	I
Exp.	1	0	0	$-\frac{1}{2d}$	$\frac{1}{2d}$	$-\frac{1}{2d}$	0	0	0	$\frac{2d-1}{2d}$	1	$\frac{1-2d}{2d}$	$\frac{1}{2d}$	0	1	$\frac{1}{2d}$	0

Table 1: Top table: The number of available data estimates per trait for birds and mammals. Bottom table: The theoretical exponents of body mass allometries from Witting (1995, 2017a), with $t_x \in \{t_p, t_j, t_s, t_m, t_r, t_g, t_l\}$. The spatial dimensionality (d) of the foraging behaviour is listed in Table 2.

Class	Order	Family	d
Aves	-	-	2
Mammalia	-	-	2
Mammalia	Primates	-	3
Mammalia	Carnivora	-	2
Mammalia	Carnivora	Otariidae	3
Mammalia	Carnivora	Odobenidae	3
Mammalia	Carnivora	Phocidae	3
Mammalia	Cetacea	-	3

Table 2: The spatial dimensionality (d) of the foraging behaviour is set to depend on taxonomic level, following the classification in Witting (2017a).

t_p**:** the pregnancy period in mammals, and incubation period in birds;

t_0**:** the age at birth in mammals, and the age at hatching in birds, $t_0 = 0$;

t_j**:** the age at weaning in mammals, and the age at fledging in birds;

t_i**:** the age of independence from parents, $t_j \leq t_i < t_m$ with t_m being the age of reproductive maturity;

w**:** the average body mass of an adult individual;

w_x**:** the mass at $t_x = t_0$, t_j or t_i, with relative mass $\acute{w}_x = w_x/w$.

The growth of an individual—as measured by relative mass ($\acute{w}_a = w_a/w$) over age (a)—is estimated by a Gompertz (1832) growth model

$$\acute{w}_a = \acute{w}e^{-\gamma_b e^{-\gamma_a (a-t_p)}} \tag{1}$$

where $\acute{w} = \acute{w}_j / \min(\acute{w}_j, 0.95)$ to account for cases where the mass at weaning/fledging is larger than adult mass. The parameters of the growth model (γ_a and γ_b) are estimated by the growth curve that passes through $\acute{w}_0$ at $a = t_0$, and $\acute{w}_j$ at $a = t_j$. Assuming that parents invest at least 80% in the mass of offspring, the relative mass at independence is estimated as $\acute{w}_i = \max(\acute{w}_j, 0.8)$, with t_i being the solution to the growth curve at $\acute{w}_i = \acute{w}e^{-\gamma_b e^{-\gamma_a (t_i - t_p)}}$.

2.2 Demography

The demographic traits include

p_{ad}**:** the annual survival probability of adults;

q_{ad}**:** the annual mortality of adults, $q_{ad} = 1 - p_{ad}$;

t_s**:** female age of sexual maturity;

t_m**:** female age of reproductive maturity, $t_m = t_s + t_p$;

t_r**:** the expected reproductive period for females that survive to t_m, as $t_r = 1/q_{ad}$ by appendix eqn 4;

t_g**:** generation time as the average age of reproduction, as $t_g = t_m + p_{ad}/q_{ad}$ by appendix eqn 7;

t_l**:** the maximum lifespan of an individual;

l_m**:** the probability that a new-born will survive to t_m, estimated as $l_m = 2/R$ by eqn 2;

l_r**:** the probability that an adult will survive the expected reproductive period, $l_r = {p_{ad}}^{t_r}$;

m**:** the average number of offspring produced per female per year, i.e., $m = m_b\, m_f$ where m_b is the average brood size and m_f the average brood frequency, with m_f being the inverse $m_f = 1/m_i$ of the average brood interval m_i; and

R**:** expected lifetime reproduction as the average number of offspring produced over the expected reproductive period for females that survive to t_m, estimated as $R = t_r m$.

These parameters are estimated for stable populations with a per-generation growth rate of unity

$$\lambda = l_m t_r m/2 = 1. \tag{2}$$

2.3 Life history energetics

Traits that link the demographic parameters to the energetics of the organism include

$\underline{\beta}$**:** basal mass-specific metabolism (SI unit W/g);

β**:** field mass-specific metabolism (SI unit W/g);

$\tilde{\beta}$**:** metabolic pace (SI unit Hz), defined as $\tilde{\beta} = \beta/W$, i.e., the frequency of the metabolic work $W = 1$J/g that is carried out when one joule is metabolized per gram of tissue;

α **:** the handling of net resource assimilation (resource handling in short, SI unit J), defined as the net energy that is generated per metabolic pace, and estimated as $\alpha = \epsilon/\tilde{\beta}$. Handling is a joint parameter ($\alpha = \grave{\alpha}\rho$) of intrinsic handling ($\grave{\alpha}$) multiplied by the density of the resource (ρ);

ϵ**:** the net assimilated energy that is available for reproduction is parameterised as a product $\epsilon = \alpha\tilde{\beta}$ (SI unit W) between the handling of the resource (α) and the pace of handling ($\tilde{\beta}$). It is estimated as $\epsilon = w_e\acute{\beta}R/t_r$ from eqn 3;

ϵ_g**:** relative to net energy, the gross assimilated energy includes also energy used for metabolism, growth, and self-maintenance. It is estimated as $\epsilon_g = \epsilon/2 + w\beta$ from appendix eqn 17 (SI unit W), and presented as a relative measure $\acute{\epsilon}_g = \epsilon_g/\epsilon$ of gross over net energy; and

w_ϵ**:** body mass measured by combustion energy (SI unit J); calculated as $w_\epsilon = c_{w\to d}c_{d\to\epsilon}w$ where w is mass in grams, $c_{w\to d}$ is the conversion of wet to dry organic matter [set to 0.40 for birds (Mahoney and Jehl 1984), and 0.35 for mammals (Prothero 2015)], and $c_{d\to\epsilon}$ is the conversion of dry organic matter to energy [set to 22.6 kJ/g based on Odum et al. (1965) and Griffiths (1977)].

Net energy defines lifetime reproduction by the number of fully growth offspring that it produces. Assuming complete parental investment until t_i, we have

$$R = \epsilon t_r/\acute{\beta}w_\epsilon \tag{3}$$

where

$$\acute{\beta} = (w_i + t_e\beta\bar{w}_i)/w \tag{4}$$

is a scaling parameter that scales w_ϵ to the mass at independence (w_i) and accounts for the energy that is metabolised by the offspring during the period of parental care ($t_e = t_p + t_i$), with $t_e\beta\bar{w}_i$ being the energy that is metabolised by the offspring during t_e, assuming constant mass-specific metabolism (β) and an average size

$$\bar{w}_i = \frac{1}{t_e}\int_{a=-t_p}^{t_i} w_a\, da \tag{5}$$

that is calculated by the growth model of eqn 1, with $-t_p$ being the negative age at fertilisation.

2.4 Population ecology

Important population ecological components include

N**:** population density (abundance), as the number of animals per km^2;

b**:** the standing biomass of the population, as $b = wN$ in kg/km^2;

ϵ_n**:** the energy consumption by the population, calculated as $\epsilon_n = \epsilon_g N$ (in W/km^2);

h**:** the average home range of an individual (in km^2);

h_o**:** the average home ranges overlap, calculated as the average home range divided by the average availability of space ($1/N$);

v**:** the frequency of competitive encounters per individual per unit home range overlap, given as a relative measure that is estimated as $v \propto v_f/l_f$, where $l_f \propto h^{1/d}$ is the length of foraging tracks (assumed proportional to the dth root of the d-dimensional home range) and $v_f \propto \beta_\beta w^{1/2d}$ is the average speed of foraging on those tracks, as expected from allometric correlations with β_β being the intercept of the metabolic allometry $\beta = \beta_\beta w^{-1/2d}$ (Witting 1995, 2017a); and

I**:** intra-specific interference competition per individual approximated as a relative measure $I \propto h_o v \propto Nhv$ that is obtained by multiplying the home range overlap with the frequency of competitive encounters per individual per unit home range overlap (Witting 1995, 2017a). All estimates of I are rescaled to obtain a log value ($\iota = \ln I$) of unity for the median across all species of birds.

2.5 Data

I use published data only, and all trait estimates that I obtain from the literature are treated as raw data. My broader definition of data include also the traits of a species that are calculated from the raw data of that species.

	β	$\underline{\beta}$	t_m	t_l	t_i	t_j	m	p_{ad}	q_{ad}	N	h
q_g	2.60	3.46	3.19	0.05	1.12	0.23	2.60	0.05	0.52	0.88	0.21
q_n	77.3	12.3	20.6	100.0	38.8	35.8	25.3	70.6	17.5	37.6	25.3
q_x	1.00	1.05	0.48	0.70	0.33	0.54	0.33	0.46	1.00	0.48	0.84
$\hat{x}$	−0.25	−0.24	0.01	0.14	0.04	0.14	0.00	−0.11	0.08	−0.31	1.02
σ	0.34	0.34	1.07	1.46	0.40	0.69	0.95	0.75	0.89	4.25	3.19
$\hat{x}$	−0.27	−0.28	0.13	0.13	0.08	0.15	−0.09	0.11	−0.18	−0.35	0.72
σ	0.21	0.20	0.42	0.65	0.20	0.36	0.75	0.65	0.80	1.66	1.69
$\hat{x}$	−0.26	−0.27	0.23	0.21	0.13	0.20	−0.16	0.11	−0.23	−0.35	0.97
σ	0.19	0.20	0.57	0.50	0.11	0.19	0.79	0.08	0.22	0.56	0.89
$\hat{x}$	−0.32	−0.28	0.22	0.22	0.18	0.24	−0.16	0.08	−0.21	−0.55	1.20
σ	0.03	0.03	0.01	0.00	0.00	0.03	0.03	0.00	0.00	0.18	0.05
cv	0.13	0.11	0.13	0.23	0.05	0.10	0.13	0.11	0.20	0.85	1.14
n	634	585	2480	3557	3698	3179	3138	660	660	1653	343
cv	0.14	0.14	0.21	0.28	0.10	0.18	0.23	0.16	0.23	0.97	1.10
n	415	405	486	591	675	595	596	338	338	609	254
cv	0.23	0.20	0.23	0.26	0.19	0.28	0.28	0.18	0.35	1.44	1.56
n	61	63	42	42	60	57	57	60	60	50	43
cv	0.30	0.23	0.54	0.29	0.11	0.38	0.27	0.18	0.32	1.25	2.54
n	10	10	6	6	4	3	2	9	9	14	10

Table 3: **Missing value estimation.** The q_g, q_n and q_x parameters of eqns 7 and 8 that gave the most precise estimation of missing values for the different mass-dependent traits. $\hat{x}$ is the average, and σ the standard deviation, of the data estimated allometric exponents at the different taxonomic levels (blue:genus; green:family; yellow:order; red:class). The precision of an estimated missing value is given by a coefficient of variation (cv) that is estimated from the missing value predictions of n data points.

Taxonomies and names were obtained from Wilson and Reeder (2005) for mammals and from Gill and Donsker (2014) for birds, and body masses were obtained primarily from Smith et al. (2004) for mammals and Dunning (2007) for birds. Primary data on basal metabolism were obtained from McNab (2008) for mammals and McKechnie and Wolf (2004) for birds, with field metabolic rates from Hudson et al. (2013). Data for parameters on reproduction, time periods, and individual growth were obtained from a variety of sources including Jetz et al. (2008), De Magalhães and Costa (2009), Jones et al. (2009), and Myhrvold et al. (2015). I conducted an independent literature search for annual survival rates across all major taxa of birds and mammals, with major data sources including McCarthy et al. (2008), DeSante and Kaschube (2009), Ricklefs et al. (2011), del Hoyo et al. (1992–2011), and Wilson and Mittermeier (2009–2014). Population densities were obtained from Damuth (1987) and Santini et al. (2018), and home range areas from Tucker et al. (2014), Tamburello et al. (2015), and Nasrinpour et al. (2017) with a separate literature search for bats and marine mammals.

Some of the data in these publications are the same. I determined the value of a trait for a species as the average of the available raw data, resulting in more weight to commonly agreed estimates. Table 1 list the number of species with raw data for different traits. Data were distributed relatively evenly across the taxonomic groups that are considered separately in this paper. For the traits in Table 1, there were on average raw data for 17% of the bird species and 30% of the mammalian species, with the latter including 32% for placentals, 41% for marsupials, and 21% for bats. These data, except for body mass estimates, were checked for outliers (see outlier SI), with a total of 222 outliers removed.

I list the literature references for all raw data (in SI on data references), and for the underlying raw data when derived traits are calculated from one or two underlying traits with raw data estimates. Higher-level data that are calculated from more traits are listed as data but with no specific reference. Traits that could not be calculated from the raw data of a species had missing values that were estimated by inter-specific extrapolations.

2.6 Estimating missing values

I estimated missing values by inter-specific body mass allometries and invariances following the allometric model of Witting (2017a), following the estimation sequence in Appendix C.

Estimation level: As my data come from many different sources, and as they have not been collected as a random sample across the different species, they are phylogenetically unevenly distributed. This means that the uncertainties of the missing value estimates will in-

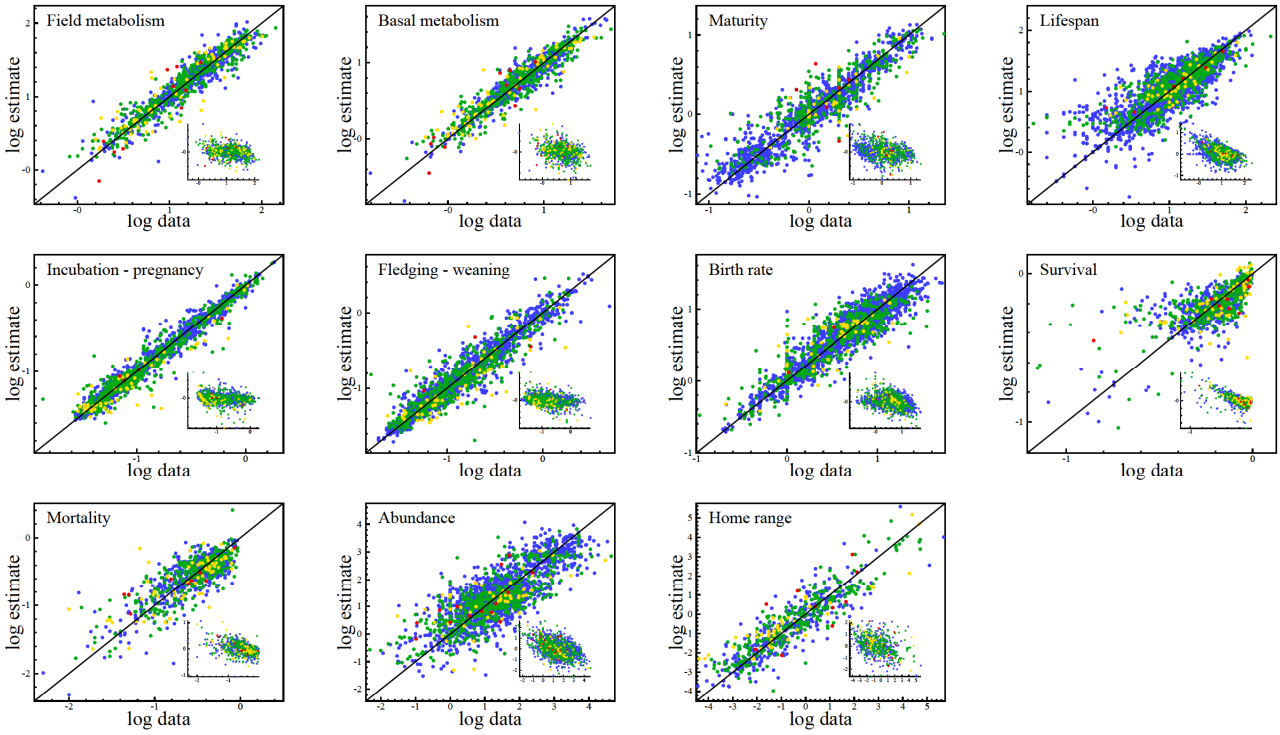

Figure 1: **Data estimation.** The estimation of missing parameters by allometric correlations was tested and optimised by the ability to predict the actual data; as illustrated here by the relationships between the data and their estimates on double logarithmic scale. Residuals are shown in insert plots, and the precision (cv) of the estimates are given in Table 3. Estimator levels: genus (blue), family (green), order (yellow), and class (red); with points of the latter sitting on top of the former.

crease with the phylogenetic distance to the nearest species with data. To capture this uneven distribution of uncertainties, I use a missing parameter estimator that differentiates between the different phylogenetic levels. This provides separate estimates of uncertainty for the different parameters at the different phylogenetic estimator levels. The uncertainty distribution is visualised for all parameter estimates across all species by a colour code, where data are presented in black and missing parameter estimates at the genus, family, order, and class levels are presented in blue, green, yellow, and red.

The missing values were estimated at the different taxonomic levels dependent upon the available data. The precision of an allometric estimate will generally increase with the number of data and decline with taxonomic level from genus over family and order to class. With the number of data points for any trait increasing with taxonomic level, we expect a trade-off where an estimator based on few data at a low taxonomic level will, at some point, provide a better estimate than an estimator with many data at a higher taxonomic level.

To determine the data limits—where lower-level estimators are preferred over higher-level estimators with more data—I constructed a hierarchical estimator that used the lowest taxonomic level with a given number (n_d) of data points. This number was estimated by a numerical minimization of the sum of squares of the difference between raw data and their predicted values, with the predicted data values of a species being predicted from the raw data of all other species.

Given the optimal missing value estimation of eqns 6 to 8 below, the minimization of the sum of squares between the raw data and their predicted values determined that the more precise estimates of missing values were obtained with a n_d parameter around unity. Taxonomic proximity was thus prioritized over sample size, with missing values being calculated at the lowest taxonomic level with one or more raw data of the required parameters. Genus (g) was prioritized over family (f), family over order(o), and order over class (c).

Estimator optimisation: A missing parameter value for a mass invariant parameters—like $\acute{w}_0$, $\acute{w}_j$, and

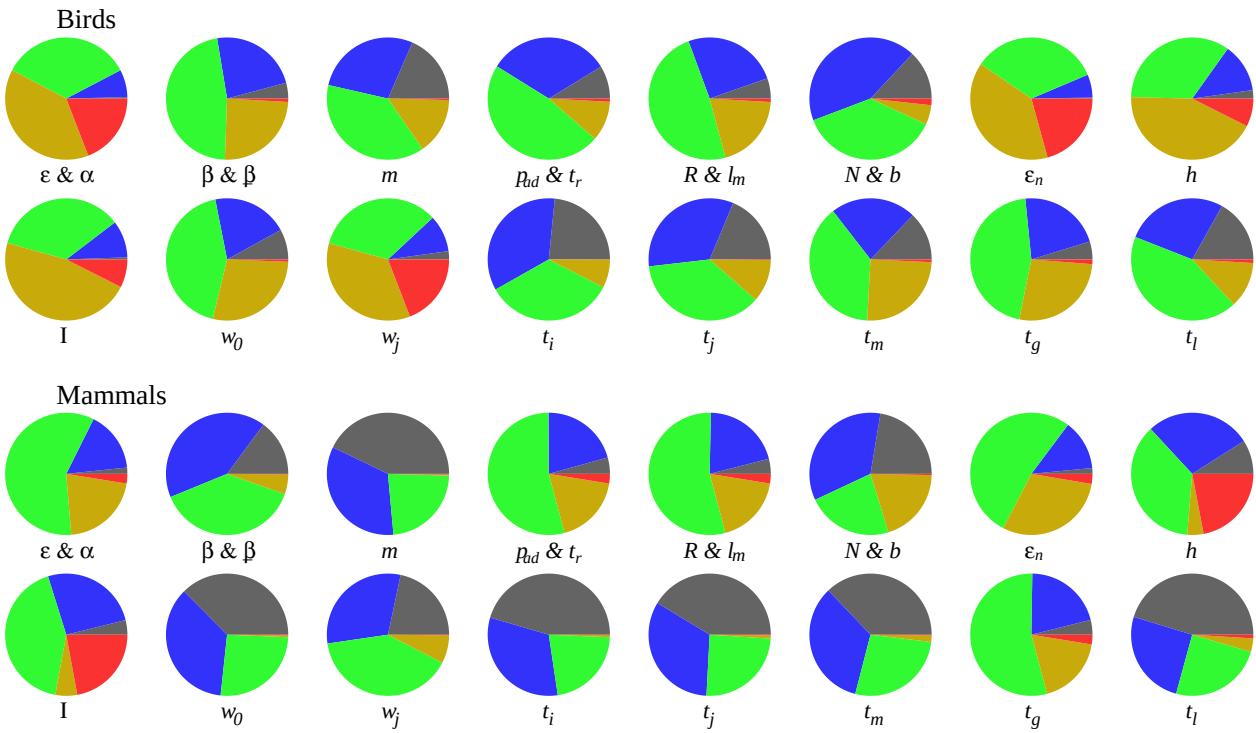

Figure 2: **Estimator distributions** for 9,488 species of birds, and 4,865 species of mammals. Estimator levels: data (black), genus (blue), family (green), order (yellow), and class (red).

l_r—was estimated as the average of the raw data across the lowest taxonomic level with raw data for that parameter. For mass-dependent parameters—like t_m, t_l, and β—the missing values were calculated as allometric functions of mass. The age of reproductive maturity, e.g., was calculated as

$$t_m(x, n) = t_{m,\circ} w^{\hat{t}_m} \tag{6}$$

with x denoting the lowest taxonomic level with raw data, and n the number of data points at that level. The allometric exponent ($\hat{t}_m$) and intercept ($t_{m,\circ}$) were estimated as a joint function

$$\begin{aligned} \hat{t}_m &= q\,\hat{t}_{m,D} + (1-q)\,q_x \hat{t}_{m,T} \\ t_{m,\circ} &= q\,t_{m,\circ,D} + (1-q)\,t_{m,\circ,T} \end{aligned} \tag{7}$$

of the theoretical expectations from Witting (1995, 2017a) [subscript T; e.g. $\hat{t}_{m,T} = 1/2d$ from Table 1 with ecological dimensionality (d) from Table 2] and the n data points at the xth taxonomic level [subscript D, with $\hat{t}_{m,D}$ and $t_{m,\circ,D}$ being point estimates from a linear regression on double logarithmic scale]. The weight

$$q = 1 - e^{-e^{-q_g(n-q_n)}} \tag{8}$$

of the data estimate increases monotonically from zero to one as a function of n, except for $n \leq 3$ cases where the exponent ($\hat{t}_m = q_x \hat{t}_{m,T}$) was proportional to the theoretical expectation and the $t_{m,\circ}$ intercept of eqn 6 was the average allometric intercept for the n species given the $\hat{t}_m$ exponent.

The three parameters q_g, q_n, and q_x were estimated separately for all allometrically dependent life history parameters. This was done by a numerical minimization of the sum of squares (across species with data) for the difference between the raw data and the predicted values by the estimators at the lowest taxonomic levels, given the data of all the other species.

Given estimators at the lowest taxonomic level with data, the optimal values of the parameters for eqns 7 and 8 are listed in Table 3. They follow a general pattern where missing parameters are calculated from the theoretical exponents for estimators with few available data. With an increased number of data there is an often steep transition to a fully empirically based estimator, with the average values of the empirically estimated exponents listed in Table 3, for estimators at the genus (blue), family (green), order (yellow), and class (red) level.

The average precision (cv) of the missing parameter

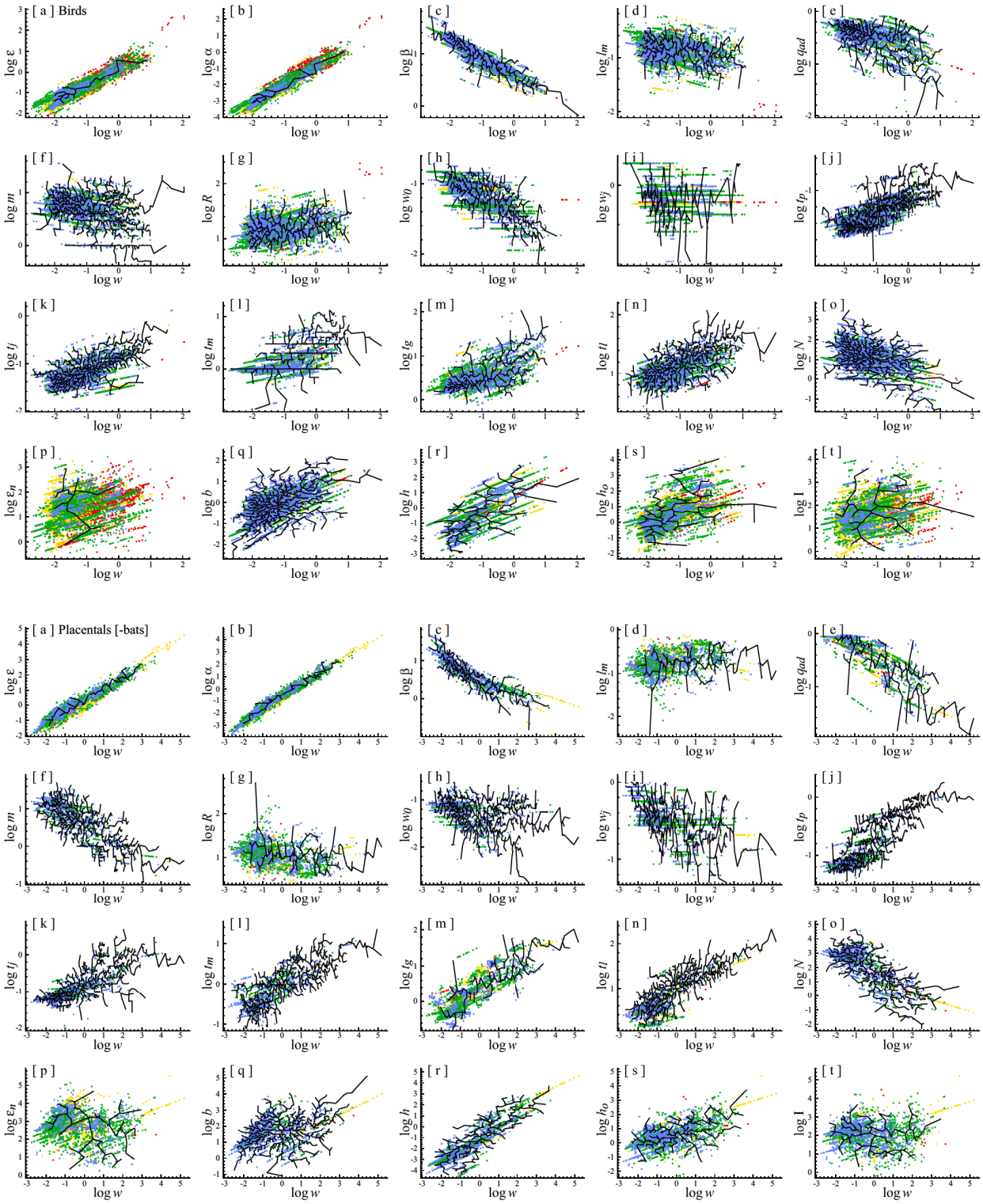

Figure 3: **Allometric scaling.** Birds in the top four rows, placental mammals in the bottom four. The black lines outline data, and the coloured dots estimates at different levels. Estimator levels: data (black), genus (blue), family (green), order (yellow), and class (red); with points of the latter sitting on top of the former.

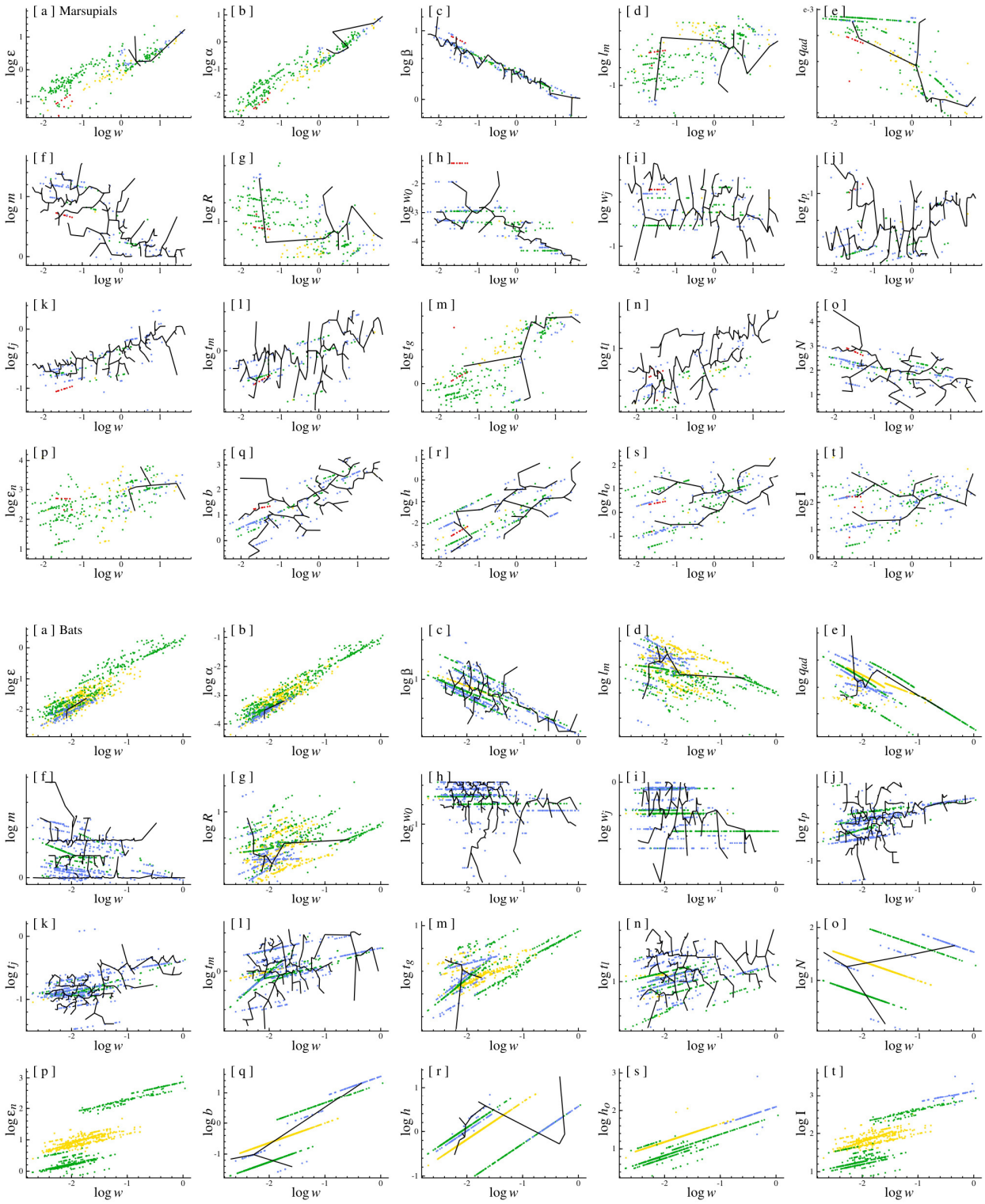

Figure 4: **Allometric scaling.** Marsupial mammals in the top four rows, bats in the bottom four. The black lines outline data, and the coloured dots estimates at different levels. Estimator levels: data (black), genus (blue), family (green), order (yellow), and class (red); with points of the latter sitting on top of the former.

Trait	w	w_0	w_j	t_p	t_j	γ_a	γ_b	t_m	t_r	t_g	t_l	l_m	p_{ad}	m	R
Unit	kg	–	–	y	y	–	–	y	y	y	y	p	p	$\frac{1}{y}$	$\frac{1}{t_r}$
Coppery Ringtail *Pseudochirops cupreus*	$^{a:c:d}$ 1.8	.00023	.24	.044	.5	3.5	9.8	1.4	4.1	4.6	5.6	.45	.76	1.1	4.5
San Quintin Kangaroo Rat *Dipodomys gravipes*	$^{a:c:d}$ .084	.068	.39	.083	.073	14	8.9	.28	1.2	.51	6.6	.32	.19	5.1	6.3
Buff-bellied Rhipidomys *Rhipidomys ochrogaster*	$^{a:c:d}$ .089	.071	.36	.074	.062	15	8	.25	1.5	.71	4.6	.1	.32	13	19
Chiapan Climbing Rat *Tylomys bullaris*	$^{a:c:d}$ .28	.071	.16	.11	.073	5	4.6	.29	1.7	.98	5.6	.086	.41	14	23
Greater Forest Shrew *Sylvisorex ollula*	$^{a:c:d}$ .015	.068	.77	.065	.063	37	30	.3	1.2	.48	2.8	.12	.15	14	16
Seychelles Flying Fox *Pteropus seychellensis*	$^{a:c:d}$ .48	.14	.51	$^{c:d}$ .43	.37	2.9	6.9	1.6	6.8	7.4	^{d} 9.9	.3	.85	$^{c:d}$ 1	6.8
Hairy Little Fruit Bat *Rhinophylla alethina*	^{d} .0069	.16	.65	.32	.12	12	100	.82	3	2.8	10	.66	.67	1	3
Thumbless Bat *Furipterus horrens*	$^{a:c:d}$ .0032	.18	.65	.22	.099	14	33	.85	4.8	4.7	12	.41	.79	1	4.9
Sechuran Fox *Lycalopex sechurae*	$^{a:c:d:e}$ 4.1	.02	.17	.15	.18	4.4	7.6	.86	2.5	2.3	^{d} 9.9	.18	.59	4.5	11
Atlantic White-sided Dolphin *Lagenorhynchus acutus*	$^{a:c:d:e}$ 190	$^{c:d}$ .13	.34	$^{c:d}$ .87	$^{c:d}$ 1.5	.43	3	^{e} 6.1	25	30	31	.16	.96	$^{c:d:e}$ .5	12
Shy Albatross *Thalassarche cauta*	$^{b:d}$ 4	.047	1.1	^{d} .19	^{d} .4	10	23	10	14	24	^{d} 40	.28	.93	^{d} .5	7.2
Barolo Shearwater *Puffinus baroli*	^{d} .19	.1	1.1	^{d} .14	^{d} .2	20	38	4.8	10	14	^{d} 19	.19	.9	^{d} 1	10
Long-legged Buzzard *Buteo rufinus*	$^{b:d:e}$ 1.2	.042	.99	^{d} .09	^{d} .13	32	61	^{d} 2	5.9	6.9	^{d} 8.5	.11	.83	$^{d:i}$ 3	18
Arabian Scops Owl *Otus pamelae*	^{d} .069	.098	.93	.067	.068	52	74	.96	3.6	3.5	9.5	.15	.72	3.7	13
Social Flycatcher *Myiozetetes similis*	$^{b:d}$ .028	.11	.91	^{d} .042	^{d} .058	56	24	1	2.4	2.4	9	.14	.58	6	14
Orange-crowned Fairywren *Clytomyias insignis*	$^{b:d}$ .012	.082	.81	.037	.035	69	32	1	2.8	2.8	11	.12	.64	6	17
Yellow-throated Greenbul *Arizelocichla chlorigula*	^{d} .035	.072	.81	.036	.036	69	30	1.1	2.3	2.4	10	.14	.56	6.3	14
Goulds Shortwing *Heteroxenicus stellatus*	$^{b:d}$ .023	.099	1.1	.038	.04	96	93	1	2	2	8.9	.14	.5	7.2	14
Altai Accentor *Prunella himalayana*	$^{b:d}$ .027	.082	.81	.035	.036	69	28	1	3.4	3.4	13	.068	.7	8.8	30
Stripe-tailed Yellow Finch *Sicalis citrina*	$^{b:d}$ .012	.097	.81	.034	.035	68	24	.91	2.6	2.5	9.4	.17	.61	4.7	12

Table 4: Growth and demography for 20 randomly chosen mammal and bird species. Estimator levels: data (black), genus (blue), family (green), order (yellow), and class (red). The superscript letters for data refer to references in the SI on data references.

estimates are also listed in the table. Excluding the estimator for abundance (N) and home range (h), the precisions are generally acceptable for all estimators. The average cv is 0.23, with a range that varies from 0.05 to 2.54. Precision is generally declining with an increase in the taxonomic level of the estimator, with the average cv being 0.21 at the genus level, 0.32 at the family level, 0.44 at the order level, and 0.72 at the class level.

The underlying relationships between the raw data and their values as predicted by the optimal estimators are show Fig. 1. There is a close to linear dependence for all traits, except that the maximum lifespan and survival estimators tend to overestimate for small body masses.

3 Results

3.1 Estimation level & space

The proportions of the different parameter estimator levels are shown in Fig. 2. Mammals have a larger fraction of data than birds for most traits, yet even for birds 85%, 93%, 92%, 89%, 74%, and 87% of the estimates for m, N (and b), t_p, t_j, t_m and t_l are at or below the family level. The corresponding values are 100%, 88%, 99%, 99%, 98%, and 95% for mammals, where 43%, 22%, 45%, 41%, 37%, and 45% of the estimates are data.

For mass-specific metabolism 4% and 15% of the estimates for birds and mammals are data, and 74% and 95% are at or below the family level. For $t_r = 1/q_{ad}$, 9% and 4% of the estimates for birds and mammals are

Trait	w	α	$\underline{\beta}$	β	ϵ	$\acute{\epsilon}_g$	N	b	ϵ_n	h	h_o	v	I
Unit	kg	J	$\frac{W}{kg}$	$\frac{W}{kg}$	W	–	$\frac{1}{km^2}$	$\frac{kg}{km^2}$	$\frac{W}{km^2}$	km^2	–	–	–
Coppery Ringtail *Pseudochirops cupreus*	$^{a:c:d}$ 1.8	.2	2.2	5	1	9.2	130	220	1200	.02	2.6	46	120
San Quintin Kangaroo Rat *Dipodomys gravipes*	$^{a:c:d}$ .084	.011	5.7	19	.21	7.9	820	69	1400	.0033	2.7	94	260
Buff-bellied Rhipidomys *Rhipidomys ochrogaster*	$^{a:c:d}$ .089	.028	7.4	23	.65	3.6	120	11	280	.0029	.35	120	43
Chiapan Climbing Rat *Tylomys bullaris*	$^{a:c:d}$ .28	.11	5.2	16	1.7	3.2	840	230	4500	.0036	3	140	430
Greater Forest Shrew *Sylvisorex ollula*	$^{a:c:d}$ .015	.0027	15	33	.088	6.2	960	15	530	.0014	1.3	110	140
Seychelles Flying Fox *Pteropus seychellensis*	$^{a:c:d}$ .48	.042	3.3	25	1	12	45	21	550	2	88	12	1100
Hairy Little Fruit Bat *Rhinophylla alethina*	^{d} .0069	.00017	10	35	.0061	40	26	.18	6.4	.48	13	4.2	53
Thumbless Bat *Furipterus horrens*	$^{a:c:d}$ .0032	7.2e-5	11	35	.0025	44	35	.11	3.9	.25	8.7	3.9	34
Sechuran Fox *Lycalopex sechurae*	$^{a:c:d:e}$ 4.1	1.5	2.7	6.6	10	3.2	1.5	5.9	47	5.5	8	5.7	45
Atlantic White-sided Dolphin *Lagenorhynchus acutus*	$^{a:c:d:e}$ 190	54	1.6	4.3	230	4	1.1	210	1100	92	100	5.5	570
Shy Albatross *Thalassarche cauta*	$^{b:d}$ 4	.24	2.2	7.4	1.8	17	2.3	9.3	71	25	59	2.9	170
Barolo Shearwater *Puffinus baroli*	^{d} .19	.012	5.5	24	.3	16	7.5	1.5	37	.84	6.3	12	74
Long-legged Buzzard *Buteo rufinus*	$^{b:d:e}$ 1.2	.2	3	8.2	1.7	6.3	2.2	2.6	23	6.2	14	3.6	49
Arabian Scops Owl *Otus pamelae*	^{d} .069	.015	5.9	5.9	.085	5.2	3.6	.25	1.6	.49	1.8	2.2	3.9
Social Flycatcher *Myiozetetes similis*	$^{b:d}$ .028	.0026	13	41	.11	11	^{bd} 4.4	.12	5.2	.045	.2	32	6.3
Orange-crowned Fairywren *Clytomyias insignis*	$^{b:d}$ .012	.00067	18	46	.031	19	91	1.1	53	.029	2.6	30	78
Yellow-throated Greenbul *Arizelocichla chloriguia*	^{d} .035	.0028	8.7	26	.073	13	89	3.1	84	.085	7.5	17	130
Goulds Shortwing *Heteroxenicus stellatus*	$^{b:d}$ .023	.0029	14	40	.12	8.4	24	.55	23	.011	.25	59	15
Altai Accentor *Prunella himalayana*	$^{b:d}$ .027	.0019	18	55	.11	14	85	2.3	130	.064	5.5	35	190
Stripe-tailed Yellow Finch *Sicalis citrina*	$^{b:d}$ .012	.00045	18	55	.025	26	12	.14	8	.027	.34	36	12

Table 5: Energetics and population ecology for 20 randomly chosen mammal and bird species. Estimator levels: data (black), genus (blue), family (green), order (yellow), and class (red). The superscript letters for data refer to references in the SI on data references.

data, and 89% and 79% are at or below the family level. The mass at birth ($\acute{w}_0$) and weaning ($\acute{w}_j$) have a strong data base in mammals (37% & 22% are data), but less so in birds especially for mass at fledging (8% & 2% are data).

Traits that are less supported by data are typically calculated from at least two independent parameters, with estimator levels given by the parameter that is estimated at the highest taxonomic level. These traits include ϵ, α, R, l_m, ϵ_n, I, and t_g. Yet, even net energy (ϵ) and resource handling (α)—which are calculated from seven underlying parameters—have 42% and 76% of the estimates in birds and mammals at or below the family level.

The estimated life history variation is plotted as allometric functions of body mass for birds and placentals in Fig. 3 and marsupials and bats in Fig. 4. The black lines in the plots connect data, forming trees that illustrate the parameter space of the data. The estimated parameters for individual species are plotted by dots, with the taxonomic level of the estimator indicated by colour. The dots show that the extrapolation of parameters across species are contained within the overall parameter space of the data.

This is true especially for traits with many data, where the black trees cover almost the complete parameter space of the estimates. Yet, narrow extrapolation areas exist, like the line of order-level dots (yellow) for the allometric scaling of metabolism (β) in larger mammals. The parameters with fewer data have large data free areas that are dominated by especially order and family level estimators. Yet, even these extrapolation

Trait	w	ϵ	$\underline{\beta}$	α	m	t_m	t_r	q_{ad}	R	N	b	ϵ_n	h	h_o	ι
Unit	g	W	$\frac{\text{W}}{\text{kg}}$	J	y^{-1}	y	y	y^{-1}	t_r^{-1}	km^{-2}	$\frac{\text{kg}}{\text{km}^2}$	$\frac{\text{W}}{\text{km}^2}$	km^2	-	-
Birds	$36^{1,000}_{2.2}$	$.097^{1.5}_{1.9}$	$12^{3.9}_{.79}$	$.0027^{0.15}_{2.8}$	$5.6^{3.9}_{.69}$	$1^{1.8}_{.55}$	$2.6^{4.8}_{.64}$	$.38^{0.21}_{.64}$	$15^{19}_{.62}$	$14^{4}_{1.9}$	$.68^{4}_{2.2}$	$24^{-}_{1.8}$	$.12^{5.6}_{3.3}$	2.1^{23}_{3}	1^{-}_{2}
Plac.	$130^{1,000}_{3.7}$	$.56^{2.1}_{2.8}$	$4.9^{3.3}_{1.1}$	$.035^{0.25}_{3.8}$	$7.5^{3.8}_{1.4}$	$.52^{0.92}_{1.3}$	$1.6^{2.8}_{.94}$	$.63^{0.36}_{.94}$	$13^{11}_{.79}$	$390^{55}_{3.5}$	$39^{55}_{2.4}$	$640^{-}_{2.4}$	$.005^{0.068}_{4.5}$	$2.3^{3.7}_{2.5}$	2.3^{-}_{2}
Mars.	$360^{1,000}_{2.9}$	$.9^{1.5}_{1.8}$	$3.1^{2.3}_{.84}$	$.094^{0.23}_{2.7}$	$5.3^{3}_{1.3}$	$.84^{0.96}_{.75}$	$1.6^{2.6}_{.66}$	$.63^{0.39}_{.66}$	$8.8^{7.8}_{.7}$	$120^{75}_{1.8}$	$24^{75}_{2.8}$	$370^{-}_{2.2}$	$.027^{0.05}_{2.9}$	$3.3^{3.8}_{2.8}$	$2.2^{-}_{2.2}$
Bats	$13^{1,000}_{1.9}$	$.018^{2.6}_{2.2}$	$7.8^{3.1}_{.55}$	$.00059^{0.11}_{2.3}$	$1.3^{1.1}_{.43}$	$1^{2}_{.61}$	$3.6^{7}_{.39}$	$.27^{0.14}_{.39}$	$5.3^{7.6}_{.41}$	$18^{44}_{1.1}$	$.22^{44}_{2.6}$	$7.2^{-}_{2.5}$	$.9^{2.6}_{.98}$	$14^{110}_{1.2}$	$1.3^{-}_{1.8}$

Table 6: Inter-specific medians of selected traits covering all models for birds, placentals (Plac.), marsupials (Mars.), and bats. Superscript values are allometric intercepts listing expected trait values for body masses of 1kg, and subscripts are the order of magnitudes of the 95% ranges of the inter-specific distributions (the latter calculated for $I = e^{\iota}$ for the level of interference).

areas tend to be contained within the space of widely scattered data.

3.2 Life history variation

The estimated models for 20 randomly chosen species are listed in Table 4 for the growth and demographic related parameters, and in Table 5 for the energetic and population ecology related parameters. The complete sets of models for 9,488 birds and 4,865 mammals are listed in the SI. These estimates illustrate a diversity of life histories and, to describe the variation and analyse their evolution, Table 6 summarises the median values of selected traits for birds, placentals (minus bats), marsupials, and bats (BPMB). Included in the table are also estimates of the allometric intercepts representing the expected traits of similar sized species of 1kg, as well as the 95% ranges of the inter-specific variation of the four taxa.

Body mass & net energy: The trait variation across and within the four taxa reflects underlying natural selection variation, with the selected inter-specific range in body mass covering 4.8, 6.4, 3.9, and 2.7 orders of magnitude for BPMB, and the corresponding 95% ranges covering 2.2, 3.7, 2.9, and 1.9 orders of magnitude. The median marsupial is 177% larger than the median placental that is 261% larger than the median bird that is 177% larger than the median bat.

Given population dynamic feed-back selection, the body mass (w) of a species is selected primarily by the interactive competition that follows from the population dynamic growth that is imposed by the available net energy (ϵ) of the individuals in the population, with the selected variation in body mass reflecting the underlying variation in net energy. This selection predicts an allometric relation of $\epsilon \propto w^{3/4}$ (Witting 2017a; with the proportional relation being between body mass and net energy on the per-generation timescale of natural selection), with the 95% body mass ranges calculated from the allometry given the 95% ranges in net energy covering 107%, 106%, 75%, and 150% of the observed body mass ranges in BPMB. This lack of a 100% match is expected, as additional body mass variation is selected from allometrically uncorrelated variation in the survival of adults and offspring (Witting 2023).

The w/ϵ ratio of the medians are 0.37, 0.23, 0.40, and 0.72 for BPMB, implying that bats are naturally selected for a more efficient conversion of net energy to mass relative to the other taxa. Marsupials and birds are medium efficient, and placentals least efficient. We will take a closer look at this efficiency when we examine the demographic traits below.

With the net energy of a species ($\epsilon = \alpha\beta$) following from the product between resource handling (α) and the pace of handling (β), the inter-specific variation in body mass and net energy reflects underlying variation in resource handling and mass-specific metabolism. With mass-specific metabolism in birds and mammals approximating Kleiber (1932) scaling with allometric exponents around $-1/4$, the 95% ranges of mass-specific metabolism cover 36%, 30%, 29%, and 29% of the 95% ranges of body mass for BPMB. With the $-1/4$ power decline in mass-specific metabolism with an increase in mass being predicted as a secondary mass-rescaling selection that is imposed by the selection of mass (Witting 2017a), the primary contributor for the selected variation in body mass is the underlying variation in resource handling, reflecting variation in the ways that species handle their resources as well as variation in the density of resources. The downscaling of mass-specific metabolism ($\beta \propto w^{-1/4}$) during the selection of mass generates a decline in net energy in physical time ($\epsilon = \alpha\beta \propto w^{-1/4}$ given constant α), but it maintains net energy on the per-generation timescale of natural selection ($\epsilon t_r \propto w^0$ given constant α) as it

includes a corresponding dilation ($t_r \propto 1/\beta \propto w^{1/4}$) of natural selection time. Thus, other things being equal, the body mass within a taxa is selected in proportion with resource handling ($w \propto \alpha$) with the α/w ratios of the 95% ranges of the inter-specific distributions being 1.27, 1.03, 0.93, and 1.21 for BPMB. These ratios are closer to the other-things-being-equal-value of unity than the corresponding $\epsilon^{4/3}/w$ ratios for net energy given above. The larger α/w ratio for birds, however, is the exception that reflects a smaller (-0.33; Witting 2023) than expected ($-1/4$) allometric exponent for mass-specific metabolism. This stronger negative scaling in birds implies an additional decline in the pace of handling with increased mass and thus a stronger than proportional dependence of mass on resource handling.

The median β/α ratios are 4400, 140, 33, and 13000 for BPMB, which means that mass-specific metabolism is much more important for the generation of net energy in bats and birds than in placentals and marsupials. If we examine the corresponding β/α ratios at the allometric intercept (26, 13, 10, & 28) we find a less extreme but similar ranking, reflecting a resource handling in bats and birds at 1kg that are only 44% and 60% of the corresponding resource handling in placentals, but also a mass-specific metabolism that is 118% larger in 1kg birds compared to placentals. The low importance of metabolism for the generation of net energy in marsupials reflects mainly a mass-specific metabolism that is 70% of the metabolism in placentals at the 1kg intercept, as resource handling in marsupials is 92% of handling in placentals at 1kg.

Demography: With demographic parameters like m, t_m, t_r, and q_{ad} being yearly rates or ages/periods in years they scale inversely with mass-specific metabolism with allometric exponents for terrestrial birds and mammals around 1/4 (Witting 1995, 2023). The 95% range of the inter-specific variation are thus about similar to the corresponding range for mass-specific metabolism, with the ratio of the average range for m, t_m, and $t_r = 1/q_{ad}$ over β being 0.79, 1.1, 1.1, and 0.87 in BPMB.

The natural selection of an efficient conversion of net energy into body mass is to a large degree determined by the survival of offspring and adults. This is because the efficiency of the feed-back selection of mass is defined by the species ability to transform net energy into the population dynamic growth that generates the density dependent interactive competition that selects net energy into mass (Witting 1997). A low survival of offspring to the age of reproductive maturity (l_m) lessens this efficiency by wasting energy on offspring that die before they reproduce, and a low adult survival (p_{ad}) implies a short reproductive period [$t_r = 1/(1 - p_{ad})$] reducing the time where adults transform energy into population growth.

The efficiency of selecting energy into mass is also reflected in the reproductive rates as these are determined primarily by the two survival rates. Owing to the per-generation equilibrium growth rate of unity ($\lambda = l_m R/2 = 1$), lifetime reproduction is inversely related to the survival of offspring to reproductive maturity ($R = 2/l_m$). And with lifetime reproduction being defined as $R = t_r m$, annual reproduction ($m = R/t_r$) is selected in proportion to the adult mortality (q_{ad}) that defines the reproduction period ($t_r = 1/q_{ad}$).

With median offspring survival (l_m) in bats being 215%, and median adult survival 161%, of the average median offspring and adult survival in birds, placentals, and marsupials, bats have by far the most efficient conversion of net energy to mass, with a median w/ϵ conversion ratio of 216% relative to the average median across the other three taxa. This is reflected in the lowest median lifetime reproduction of $5.3/t_r$, the longest median reproductive period of 3.6y, and the lowest median annual reproduction of 1.3/y.

Following bats, birds and marsupials have about similar median w/ϵ conversion efficiencies of 0.37 and 0.40, being on average 167% of the median efficiency of placentals. Yet, the ways of obtaining these median conversion efficiencies differ. Where adult bird survival is 168% of adult survival in marsupials at the median, the median survival of marsupial offspring to reproductive maturity is 164% of offspring survival in birds. This implies similar annual reproduction in the two taxa (medians of 5.6/y and 5.3/y), but a low median lifetime reproduction of $8.8/t_r$ in marsupials, compared with the largest lifetime reproduction of $15/t_r$ obtained by birds due to their relatively long median reproductive period of 2.6y following low adult survival. Having low median adult survival like marsupials, and low median offspring survival like birds, placentals have the smallest efficiency when it comes to converting net energy into mass.

Ecology: When we examine the ecological traits we note from Fig. 4 that there are hardly any pure data estimates for bats except for a few for abundance and home range, and I will thus not include bats in the comparison here.

For the remaining taxa let us examine the inter-specific 95% ranges for abundance (N), biomass (b), home range (h), and home range overlap (h_o) relative

to the expected ranges from the 95% range in body mass and the allometric expectations ($N \propto w^{-3/4}$, $b \propto w^{1/4}$, $h \propto w^1$, & $h_o \propto w^{1/4}$; we do not include ϵ_n and ι here as these are predicted to be invariant of w). This shows that the observed span in N, b, h, and h_o are 106%, 190%, 124%, and 214% larger than expected. This general within taxa overdispersal of ecological estimates relative to the allometric expectations reflects most likely not only additional ecological variation but also increased estimation uncertainty for ecological traits.

For the medians there is for most ecological traits a very large difference between birds and mammals (especially placentals) where, relative to birds, populations of placentals are 2800% more abundant, having 5700% more biomass, using 2700% more resources per unit time. Yet, the median home range of a placental in only 4.2% of the median home range of a bird. These differences remain pronounced when corrected for mass, where placentals are 1400% more abundant, with 1400% more biomass, and a home range of only 1.2% relative to birds.

These large ecological differences between birds and mammals are in sharp contrasts to the median home range overlap, which is essentially identical between the two taxa. To examine this contrast in more detail, let us compare the order of magnitude of the range in the medians across birds, placentals, and marsupials for the traits in Table 6. These between taxa orders of magnitude differences in the medians are 1 for body mass, 0.97 for net energy, 0.59 for mass-specific metabolism, and 1.5 for resource handling. The demographic traits have smaller and similar levels of variation across traits, with the average order of magnitude difference in the medians of the demographic traits being 0.22. So apart from resource handling and net energy, we find the between taxa differences in the medians to be substantially smaller than the differences in median body mass. Yet, the differences in abundance, biomass, population energy consumption, and home range are all substantially larger than the difference in body mass, with the corresponding order of magnitude differences in the medians being 1.4, 1.8, 1.4, and 1.4. This indicates a large natural selection difference in the ecology of birds and mammals, a difference that is not selected into a corresponding difference in the physiology and demographic traits.

With an order of magnitude estimate of only 0.2, the between taxa range in median home range overlap is the smallest observed range across all traits. This indicates that the spatial packing of home ranges in response to the density of the population plays a central unifying role in the natural selection of the life history and ecology as a whole, and this is the case for population dynamic feedback selection. Here, it is the density dependent trade-off between local resource exploitation and interactive competition that selects a home range overlap that optimises the foraging ecology of individuals, with the spatial dimensionality of the ecological packing of home ranges selecting the exponents of body mass allometries (Witting 1995, 2017a, 2023).

The main selection attractors of population dynamic feedback selection are competitive interaction fixpoints, where the demography and associated population growth and density regulated population abundance are selected to a balance where they generate the level of interactive competition that is pre-defined by the selection attractor of the competitive interaction fixpoint (Witting 1997). There are several competitive interaction fixpoints (Witting 2002, 2008), with the ratio in the ι-level of interference of the selection attractor of an exponentially increasing body mass over the attractor of a stable mass being 2.3, exactly as the ratio of the median estimates for placentals over birds in Table 6. Apart from the elevated interference competition—and associated increase in population abundance, biomass, and population energy consumption—that is necessary for the selection of an exponential increase in body mass, the selection mechanisms for a stable and increasing body mass are similar generating no obvious difference in the physiology and demographic traits.

3.3 Population dynamics

The 14,353 equilibrium life histories provided in this paper are base case models that are easily extended into complete population dynamic models for most species. This is exemplified in this section, where some of the models are used to explain a diverse range of population dynamic timeseries.

The population dynamics of a species depend on the age-structured demography that defines the timescale of the dynamics, and on the population dynamic regulation that defines not only the bounds on abundance but also the properties of the dynamics, let it be monotonic growth, damped to stable population cycles, fluctuating, or chaotic dynamics.

While regulation is relatively easily estimated from timeseries of abundance estimates, this is not the case for the age-structured demography. It is thus essential that the latter is available from other sources, as the life history models provided in this paper. When these models are extended into age-structured population dy-

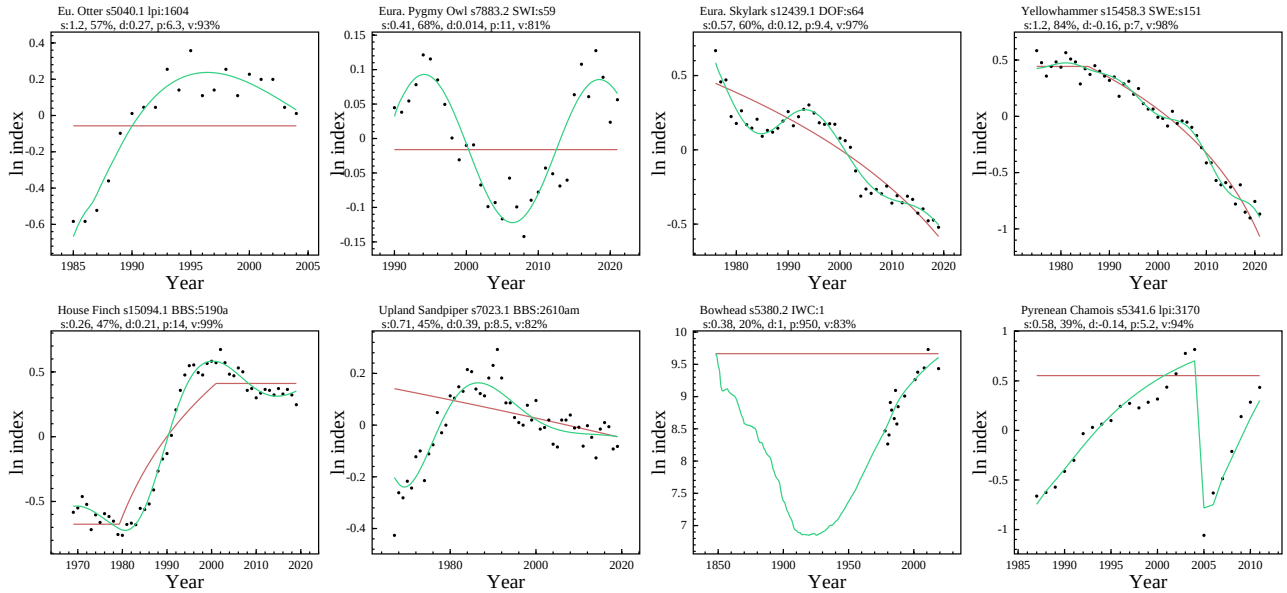

Figure 5: Examples of population dynamic models fitted to timeseries of abundance estimates (for details see the text). Dots are index series of abundance, red lines the estimated equilibria, and green curves the model trajectories. s:γ_ι & $\gamma_\iota/(\gamma_\iota+\gamma)$ in %; d:damping ratio; p:period in generations; v:explained variance.

namic models with no regulation, they project a stable population in time.

Given widespread evidence for eco-evolutionary dynamics (e.g., Thompson 1998; Sinervo et al. 2000; Hairston et al. 2005; Coulson et al. 2011; Turcotte et al. 2011a,b; Bell 2017; Hendry 2017; Brunner et al. 2019), to the equilibrium population dynamic models I add regulation by density dependent competition and regulation by population dynamic feedback selection, following Witting (2000, 2013). As described in Appendix D, this includes the addition of a density regulation parameter (γ) that regulates the growth rate as a function of the density dependent environment, and a selection regulation parameter (γ_ι) that accelerates the population dynamic growth below the equilibrium abundance and decelerates population growth above. Following Witting (2021), I use *i*) maximum likelihood statistics to estimate the two regulation parameters (and the equilibrium and initial abundance, as well as an initial measure of competitive quality) and *ii*) the Akaike information criterion (AIC, Akaike 1973) to determine if there is additional evidence for a change in equilibrium abundance or catastrophic mortality in a specific year.

Eight examples of fits to timeseries of abundance estimates are shown in Fig. 5. For these, I estimate that about 20% to 80% of total regulation is caused by selection, as measured by the $\gamma_\iota/(\gamma+\gamma_\iota)$ ratio. This generates a cyclic/over-compensatory dynamics that cannot be explained by density regulation alone. The over-compensation is illustrated by the growth of European Otter (*Lutra lutra*, from Sulkava 2006; LPI 2022) in Finland, and the Eurasian Pygmy Owl (*Glaucidium passerinum*, from Knaus and Schmid 2022) in Switzerland illustrates that populations that are both density and selection regulated have the ability to decline for longer periods below the equilibrium abundance, and to increase for longer periods above the equilibrium. Pure density regulated populations will typically only decline above the equilibrium and increase below.

Many birds that live in the farmlands of Europe have declined more or less continuously since systematic monitoring was established in several countries in the 1970th and 1980th (Gregory et al. 2019; PECBMS 2022). This is illustrated by Eurasian Skylarks (*Alauda arvensis*, from DOF 2022) in Denmark and Yellowhammers (*Emberiza citrinella*, from SFT 2022) in Sweden. The best AIC-selected models estimate that Skylark habitats in Denmark and Yellowhammer habitats in Sweden have fragmented and deteriorated by 64% and 80% since the middle of the 1970th.

Where many species suffer, others benefit from habitat changes imposed by humans. Being originally a bird of the western Unites States and Mexico, House Finches (*Haemorhous mexicanus*) established themselves in human-altered habitats throughout the Unites

States and southern Canada following a small release on Long Island in the 1940th. Across the mid-west the population was relatively stable from 1970 to 1980, followed by a large increase driven by a three-fold increase in equilibrium (most likely expansion into new habitats), according to the best AIC selected model run on data compiled (Witting 2021) from BBS (2022).

A strong increase in population need not necessarily reflect improved conditions. Being a grassland species native to the prairies of Unites States and Canada, the Upland Sandpiper (*Bartramia longicauda*) is another species that is vulnerable to habitats lost to agriculture with an increased use of pesticides. Based on the best AIC selected model run on BBS (2022) data compiled by Witting (2021), from about 1970 to 1990 Upland Sandpipers recovered by an increase of about 50% from a low abundance. Yet, the estimated habitat conditions deteriorated by about 20% from 1970 to 2020, with the species declining by about 20% from 1990 to 2020.

A longstanding treat to many species is direct anthropogenic removals, with commercial whaling in past centuries being perhaps the largest perturbation that humans have conducted ever on natural populations worldwide. The population modelling of these perturbations subtracts the historical catches from the simulated population, fitting the model trajectory to a relatively short timeseries of recent abundance estimate (Punt and Butterworth 1999; Wade 2002; Witting 2013). The bowhead whale (*Balaena mysticetus*) in the Bering-Chukchi-Beaufort Seas is one example, where the fitted model estimates that the historical catches of about $21,000$ bowheads from 1850 to 1950 (data from https://iwc.int) caused a collapse to about 1000 individuals in 1920, less than 7% of the pre-whaling abundance. From about 1910 to 1930 there was a turning point where reduced catches and increased growth (from the relaxed density regulation and selection acceleration of the depleted population) turned the population decline into an increase. With bowheads being reproductively mature around 23 years of age, it took approximately 100 years to recover to the pre-whaling abundance of about $15,000$ whales, with todays population continuing to increase.

Population perturbations may also be imposed by natural causes. The Spanish population of Pyrenean Chamois (*Rupicapra pyrenaica*) in Cerdanya-Alt Urgell increased steadily until 2005, where approximately 3,000 died from a border disease virus infection (Marco et al. 2009; data from Lopez-Martin et al. 2013; LPI 2022). This caused the population to collapse by about 80% in a single year. Yet, with Chamois being reproductively mature at about 2 years of age the population was almost recovered by 2011.

4 Discussion

I used 56,214 life history data to estimate equilibrium life history models for 14,353 species of birds and mammals. With each model having 27 parameters, 387,531 life history and ecological traits were estimated in total. This includes estimates of metabolism, net assimilated energy, individual growth, mortality, fecundity, age of reproductive maturity, generation time, life span, home range, population density, biomass, population consumption, and a relative measure of intra-specific interactive competition.

These models illustrate evolutionary differences and similarities between birds, placentals, marsupials, and bats. Differences in the survival of offspring and adults were shown to affect the w/ϵ ratio that describes the efficiency by which natural selection selects body mass from net energy. Having high offspring and adult survival, bats are most efficient with a median w/ϵ ratio is 216% of the average median for birds, placentals, and marsupials. With birds having high adult survival, and marsupials having high offspring survival, birds and marsupials are about equally efficient with median w/ϵ ratios that are 167% of the median ratio of placentals, on average. Having low adult survival like marsupials, and low offspring survival like birds, placentals were found to be least efficient when it comes to converting net energy into mass.

Ecological traits like abundance, biomass, and population energy use are much larger in mammals (especially placentals, excluding bats) compared to birds, while home ranges are much smaller. Yet, the median home range overlap is essentially identical between birds and placentals, indicating a unifying role in the natural selection of life histories. This supports the underlying theory of population dynamic feedback selection, where the density dependent trade-off between local resource exploitation and interactive competition selects a home range overlap that optimises the foraging ecology of individuals, with the spatial dimensionality of this ecological packing of home ranges selecting the exponents of body mass allometries (Witting 1995, 2017a). For a deeper analysis on the natural selection of the allometric correlations among the 14,353 species models see Witting (2023).

Another intriguing result is the estimated placental/bird ratio of 2.3 for the median ι estimate of interactive competition. This is also the theoretical value that separates species that are selected for an exponential increase in body mass (here placentals) from species

that are selected for a stable body mass (Witting 2002, 2008). The selection of an exponential like increase in at least some mammalian body masses is well documented by the fossil record (e.g., Hayami 1978; Trammer 2005; Smith et al. 2010; Okie et al. 2013), with detailed analyses of the selected increase and associated allometric correlations provided by Witting (2018, 2020).

As the majority of the estimated life history traits are inter-specific extrapolations, and as the underlying data come from many different sources, it is essential to keep in mind the uneven distribution of uncertainties, as illustrated by the colour coding of the life history estimates. Yet, the value of having complete life history models in population dynamic equilibrium for 90% of all species of birds and mammals should not be underestimated. As illustrated in Section 3.3, these life history models form base-cases that are easily extended into complete population dynamic simulations explaining a diverse range of population dynamic timeseries. The next step is the estimation of complete population dynamic models across thousands of populations, allowing for the construction of Bird and Mammal Populations (https://mrLife.org/bmp.htm) for online population dynamic analyses of all species.

5 Supplementary Information

The following supplementary files are not included in the preprint.

si_outlier.pdf: On the removal of outlier data;

si_filter.pdf: On the four estimation filters;

si_bird_demo.pdf: Demographic estimates for birds;

si_mamm_demo.pdf: Demographic estimates for mammals;

si_bird_energy.pdf: Energetic & ecological estimates for birds;

si_mamm_energy.pdf: Energetic & ecological estimates for mammals;

si_ref.pdf: Data references;

Acknowledgements

I thank all that have collected and published life history data for birds and mammals.

References

Akaike H. (1973). Information theory as an extension of the maximum likelihood principle. In: Petrov B. N. Csaki F. (eds). Second International Symposium on Information Theory: Akademiai Kiado, pp 267–281.

BBS (2022). EESC Breding Bird Survey. https://www.mbr-pwrc.usgs.gov/bbs/bbs.html.

Bell G. (2017). Evolutionary rescue. Ann. Rev. Ecol. Evol. Syst. 48:605–627.

Bonner J. T. (1965). Size and cycle. Princeton University Press, Princeton.

Brunner F. S., Deere J. A., Egas M., Eizaguirre C., Raeymaekers J. A. M. (2019). The diversity of eco-evolutionary dynamics: Comparing the feedbacks between ecology and evolution across scales. Funct. Ecol. 33:7–12.

Calder W. A. I. (1984). Size, function, and life history. Harvard University Press, Cambridge.

Charlesworth B. (1980). Evolution in age-structured populations. Cambridge University Press, Cambridge.

Coulson T., Macnulty D. R., Stahler D. R., Vonholdt B., Wayne R. K., Smith D. W. (2011). Modeling Effects of Environmental Change on Wolf Population Dynamics, Trait Evolution, and Life History. Science 334:1275–1278.

Damuth J. (1981). Population density and body size in mammals. Nature 290:699–700.

Damuth J. (1987). Interspecific allometry of population density in mammals and other animals: the independence of body mass and population energy-use. Biol. J. Linnean Society. 31:193–246.

De Magalhães J. P. Costa J. (2009). A database of vertebrate longevity records and their relation to other life-history traits. J. Evol. Biol. 22:1770–1774.

del Hoyo, J., Elliot, A., Sargatal, J., & Christie, D. A., eds (1992–2011). Handbook of the birds of the world. Vol. 1–16. Lynx Edicions, Barcelona.

DeSante D. F. Kaschube D. R. (2009). The monitoring avian productivity and survivorship (MAPS) program 2004, 2005, and 2006 report. Bird Pop. 9:86–169.

DOF (2022). Dansk Ornitologisk Forening. Punkttællinger. https://www.dof.dk.

Dunning J. B. (2007). Handbook of Avian Body Masses (2nd ed). CRC Press, Boca Raton.

Fenchel T. (1974). Intrinsic rate of natural increase: The relationship with body size. Oecologia 14:317–326.

Gill, F. & Donsker, D., eds (2014). International Ornithological Committee World Bird List (v 4.4). doi:10.14344/IOC.ML.4.4.

Gompertz B. (1832). On the Nature of the Function Expressive of the Law of Human Mortality, and on a New Mode of Determining the Value of Life Contingencies. Phil. Trans. R. Soc. Lond. 123:513–585.

Gregory R. D., Skorpilova J., Vorisek P., Butler S. (2019).

An analysis of trends, uncertainty and species selection shows contrasting trends of widespread forest and farmland birds in Europe. Ecol. Indic. 103:676–687.

Griffiths D. (1977). Caloric variation in Crustacea and other animals. J. Anim. Ecol. 46:593–605.

Hairston N. G. J., Ellner S. P., Geber M. A., Yoshida T., Fox J. A. (2005). Rapid evolution and the convergence of ecological and evolutionary time. Ecol. Lett. 8:1114–1127.

Hayami I. (1978). Notes on the rates and patterns of size change in evolution. Paleobiology 4:252–260.

Hendry A. P. (2017). Eco-evolutionary dynamics. Princeton University Press, Princeton.

Hudson L. N., Isaac N. J. B., Reuman D. C. (2013). The relationship between body mass and field metabolic rate among individual birds and mammals. J. Anim. Ecol. 82:1009–1020.

Jetz W., Sekercioglu C. H., Böhning-Gaese K. (2008). The worldwide variation in avian clutch size across species and space. PLOS Biol. 6:e303.

Jones K. E., Bielby J., Cardillo M., Fritz S. A., O'Dell J., Orme C. D. L., Safi K., Sechrest W., Boakes E. H., Carbone C., Connolly C., Cutts M. J., Foster K. J., Grenyer R., Habib M., Plaster C. A., Price S. A., Rigby E. A., Rist J., Teacher A., Binninda-Emonds O. R. P., Gittleman J. L., Mace G. M., Purvia A. (2009). PanTHERIA: a species-level database of life history, ecology, and geography of extant and recently extinct mammals. Ecology 90:2648.

Kleiber M. (1932). Body and size and metabolism. Hilgardia 6:315–353.

Knaus P., Schmid H., Strebel N., Sattler T. (2022). The State of Birds in Switzerland 2022 online. http://www.vogelwarte.ch.

Leung B., Hargreaves A. L., Greenberg D. A., McGill B., Dornelas M., Freeman R. (2020). Clustered versus catastrophic global vertebrate declines. Nature 588:267–273.

Lopez-Martin J. M., Casanovas R., Garcia-Petit J., Xifra J., Curia J., Canut J. (2013). Estatus y gestion del sarrio en el Pirineo catalan. In: Herrero J., Escuderi E., deLuco D. F., Garcia-Gonzalez R. (eds). El Sarrio Pirenaico Rupicapra p. pyrenaica: Biologia, Patologia Y Gestion: Publicaciones del Consejo de Proteccion de la Naturaleza de Aragon, pp 43–53.

LPI (2022). Living Planet Index database. www.livingplanetindex.org.

Mahoney S. A. Jehl J. R. J. (1984). Body water content in marine birds. The Condor 86:208–209.

Marco I., Rosell R., Cabezon O., Mentaberre G., Casas E., Velarde R., Lavin S. (2009). Border disease virus among Chamois, Spain. Emerg. Inf. Diseases 15:448–450.

McCarthy M. A., Citroen R., McCall S. C. (2008). Allometric scaling and Bayesian priors for annual survival of birds and mammals. Am. Nat. 172:216–222.

McKechnie A. E. Wolf B. O. (2004). The allometry of avian basal metabolic rate: Good predictions need good data. Physiolo Biochem Zool 77:502–521.

McNab B. K. (2008). An analysis of the factors that influence the level and scaling of mammalian BMR. Comp. Bioch. Physiol. A 151:5–28.

Myhrvold N. P., Baldridge E. amd Chan B., Sivam D., Freeman D. L., Ernest S. K. M. (2015). An amniote life-history database to perform comparative analyses with birds, mammals, and reltiles. Ecology 96:3109.

Nasrinpour H. R., Reimer A. A., Friesen M. R., McLeod R. D. (2017). Data preparation for West Nile Virus agent-based modelling: protocol for processing bird population estimates and incorporating ArcMap in AnyLogic. JMIR Res Protoc 6:e138.

Odum E. P., Marshall S. G., Marples T. G. (1965). The caloric content of migrating birds. Ecology 46:901–904.

Okie J. G., Boyer A. G., Brown J. H., Costa D. P., Ernest S. K. M., Evans A. R., Fortelius M., Gittleman J. L., Hamilton M. J., Harding L. E., Lintulaakso K., Lyons S. K., Saarinen J. J., Smith F. A., Stephens P. R., Theodor J., Uhen M. D., Sibly R. M. (2013). Effects of allometry, productivity and lifestyle on rates and limits of body size evolution. Proc. R. Soc. B. 280:20131007.

PECBMS (2022). Pan-European Common Bird Monitoring Scheme. https://pecbms.info.

Peters R. H. (1983). The ecological implication of body size. Cambridge University Press, Cambridge.

Prothero J. W. (2015). The design of mammals. A scaling approach. Cambridge University Press, Cambridge.

Punt A. E. Butterworth D. S. (1999). On assessment of the Bering-Chukchi-Beaufort Seas stock of bowhead whales (*Balaena mysticetus*) using a Bayesian approach. J. Cetacean Res. Manage. 1:53–71.

Ricklefs R. E., Tsunekage T., Shea R. E. (2011). Annual adult survival in several new world passerine birds based on age ratios in museum collections. J. Ornithol. 152:481–495.

Santini L., Isaac N. J. B., Ficetola G. F. (2018). TetraDENSITY: A database of population density estmates in terrestrial vertebrates. Global Ecol. Biog. 27:787–791.

Schoener T. W. (1968). Sizes of feeding territories among birds. Ecology 49:123–131.

SFT (2022). Svensk Fågeltaxering. http://www.fageltaxering.lu.se.

Sinervo B., Svensson E., Comendant T. (2000). Density cycles and an offspring quantity and quality game driven by natural selection. Nature 406:985–988.

Smith F. A., Boyer A. G., Brown J. H., Costa D. P., Dayan T., Ernest S. K. M., Evans A. R., Fortelius M., Gittleman J. L., Hamilton M. J., Harding L. E., Lintulaakso K., Lyons S. K., McCain C., Okie J. G., Saarinen J. J., Sibly R. M., Stephens P. R., Theodor J., Uhen M. D. (2010). The evolution of maximum body size of terres-

trial mammals. Science 330:1216–1219.

Smith F. A., Brown J. H., Haskell J. P., Alroy J., Charnov E. L., Dayan T., Enquist B. J., Ernest S. K. M., Hadly E. A., Jablonski D., Jones K. E., Kaufman D. M., Lyons S. K., Marquet P., Maurer B. A., Niklas K., Porter W., Roy K., Tiffney B., Willig M. R. (2004). Similarity of mammalian body size across the taxonomic hierarchy and across space and time. Am. Nat. 163:672–691.

Sulkava R. (2006). Ecology of the otter (Lutra lutra) in central Finland and methods for estimating the densities of populations. University of Joensuu, Biology PhD dissertation 0043.

Tamburello N., Cote I. M., Dulvy N. K. (2015). Energy and the scaling of animal space use. Amazoniana 186:196–211.

Thompson J. N. (1998). Rapid evolution as an ecological process. Trends Ecol. Evol. 13:329–332.

Trammer J. (2005). Maximum body size in a radiating clade as a function of time. Evolution 59:941–947.

Tucker M. A., Ord T. J., Rogers T. L. (2014). Evolutionary predictors of mammalian home range size: body mass, diet and the environment. Global Ecol. Biog. 23:1105–1114.

Turcotte M. M., Reznick D. N., Hare J. D. (2011a). The impact of rapid evolution on population dynamics in the wild: experimental test of eco-evolutionary dynamics. Ecol. Lett. 14:1084–1092.

Turcotte M. M., Reznick D. N., Hare J. D. (2011b). Experimental assessment of the impact of rapid evolution on population dynamics. Evol. Ecol. Res. 13:113–131.

Turner F. B., Jennrich R. I., Weintraub J. D. (1969). Home range and body size of lizards. Ecology 50:1076–1081.

Wade P. R. (2002). A Bayesian stock assessment of the Eastern pacific gray whale using abundance and harvest data from 1967–1996. J. Cetacean Res. Manage. 4:85–98.

Wilson, D. E. & Mittermeier, R. A., eds (2009–2014). Handbook of the mammals of the world. Vol. 1–4. Lynx Edicions, Barcelona.

Wilson, D. E. & Reeder, D. M., eds (2005). Mammals Species of the World. A Taxonomic and Geographic Reference (3rd ed). Johns Hopkins University Press, Baltimore.

Witting L. (1995). The body mass allometries as evolutionarily determined by the foraging of mobile organisms. J. theor. Biol. 177:129–137, https://doi.org/10.1006/jtbi.1995.0231.

Witting L. (1997). A general theory of evolution. By means of selection by density dependent competitive interactions. Peregrine Publisher, Århus, 330 pp, URL https://mrLife.org.

Witting L. (2000). Population cycles caused by selection by density dependent competitive interactions. Bull. Math. Biol. 62:1109–1136, https://doi.org/10.1006/bulm.2000.0200.

Witting L. (2002). From asexual to eusocial reproduction by multilevel selection by density dependent competitive interactions. Theor. Pop. Biol. 61:171–195, https://doi.org/10.1006/tpbi.2001.1561.

Witting L. (2008). Inevitable evolution: back to *The Origin* and beyond the 20th Century paradigm of contingent evolution by historical natural selection. Biol. Rev. 83:259–294, https://doi.org/10.1111/j.1469–185X.2008.00043.x.

Witting L. (2013). Selection-delayed population dynamics in baleen whales and beyond. Pop. Ecol. 55:377–401, https://dx.doi.org/10.1007/s10144–013–0370–9.

Witting L. (2017a). The natural selection of metabolism and mass selects allometric transitions from prokaryotes to mammals. Theor. Pop. Biol. 117:23–42, https://dx.doi.org/10.1016/j.tpb.2017.08.005.

Witting L. (2017b). The natural selection of metabolism and mass selects lifeforms from viruses to multicellular animals. Ecol. Evol. 7:9098–9118, https://dx.doi.org/10.1002/ece3.3432.

Witting L. (2018). The natural selection of metabolism explains curvature in allometric scaling. Oikos 127:991–1000, https://dx.doi.org/10.1111/oik.05041.

Witting L. (2020). The natural selection of metabolism explains curvature in fossil body mass evolution. Evol. Biol. 47:56–75, https://dx.doi.org/10.1007/s11692–020–09493–y.

Witting L. (2021). Selection-regulated population dynamic in birds and mammals. Preprint at bioRxiv https://dx.doi.org/10.1101/2021.11.27.470201.

Witting L. (2023). On the natural selection of body mass allometries. Acta Oecol. https://dx.doi.org/10.1016/j.actao.2023.103889.

Appendix

A Demography

I estimate the average demographic parameters for stable populations where the per-generation growth rate is unity

$$\lambda = l_m R/2 = 1 \tag{9}$$

with l_m being the probability that a new born survives to the age of maturity, and R is the expected lifetime reproduction of females that survives to t_m assuming an even sex ratio.

As data on age (a) structured reproduction is rarely available I estimate lifetime reproduction as a product

$$R = t_r m \tag{10}$$

where t_r is the expected reproductive period for females that survives to t_m, and m is the average number of offspring/births per female per year.

With $l_a = \prod_{x=0}^{a-1} p_x$ being the survival curve, the expected reproductive period is calculated as a function of adult survival (p_{ad}), where

$$\begin{aligned} t_r &= \frac{\sum_{a=t_m}^{t_l}(a+1-t_m)(l_a - l_{a+1})}{\sum_{a=t_m}^{t_l} l_a - l_{a+1}} \\ &= \sum_{a=t_m}^{t_l} l_a/l_m = \sum_{a=t_m}^{t_l} p_{ad}^{a-t_m} \\ &\approx \sum_{i=0}^{\infty} p_{ad}^i = \frac{1}{1-p_{ad}} \end{aligned} \tag{11}$$

given constant adult survival.

Data on lifespan, age of maturity, brood size and brood interval is much more common than data on survival. When data on survival is available it will usually reflect only adult survival, or some fraction of the joint survival from new-born to the age of maturity. Complete data on age-structured survival in natural populations is almost always missing. The probability to survive to the age of maturity is therefore estimated from eqn 9 as $l_m = 2/R$ given the assumption of a stable population.

Following Charlesworth (1980), a useful measure of generation time is the mean age of reproduction

$$t_g = \frac{\sum_{a=t_m}^{t_l} a\, m_a\, l_a}{\sum_{a=t_m}^{t_l} m_a\, l_a} \tag{12}$$

Assuming constant yearly reproduction (m) and constant adult survival (p_{ad}), generation time reduces to a function of the age of maturity and adult survival

$$\begin{aligned} t_g &= \frac{m\, l_m \sum_{a=t_m}^{t_l} a\, p_{ad}^{a-t_m}}{m\, l_m \sum_{a=t_m}^{t_l} p_{ad}^{a-t_m}} \\ &= t_m + \frac{\sum_{a=t_m}^{t_l}(a-t_m)p_{ad}^{a-t_m}}{\sum_{a=t_m}^{t_l} p_{ad}^{a-t_m}} \\ &\approx t_m + \frac{\sum_{i=0}^{\infty} i p_{ad}^i}{\sum_{i=0}^{\infty} p_{ad}^i} = t_m + \frac{p_{ad}}{1-p_{ad}} \end{aligned} \tag{13}$$

B Energetics

Following Witting (2002, 2017), the net energy (ϵ, given in J/s) that the female has available for reproduction is

$$\epsilon = \alpha\tilde{\beta} \tag{14}$$

where $\tilde{\beta} = \beta/W$ is metabolic pace (in 1/s), given as the frequency of the metabolic work $W = 1$J/g that is carried out when one joule is metabolized per gram of tissue, with β (in J/sg) being the field mass-specific metabolism, and α (in J) the resource handling, or net assimilated resource, per metabolic pace.

Assuming a sexual pair, the male is predicted to use the same amount of net energy in interactive competition (Witting 1997, 2002). The gender-dependent use of net energy in reproduction or interactive competition will vary between natural species; yet the fraction of the total net energy (ϵn_r) that is allocated to reproduction for a reproducing unit with n_r individuals is expected to be $\theta = 1/n_r$, i.e. 0.5 for sexually reproducing pairs.

With ϵ being the average energy that is allocated to reproduction independently of the average size of the reproducing unit, the demographic parameters are linked to net energy by the following quality-quantity trade-off

$$R = \epsilon t_r/\acute{\beta} w_\epsilon \tag{15}$$

where w_e is adult mass as combustion energy, and $\acute{\beta}$ a scaling parameter by eqn 4 assuming complete parental investment until the age of independence (t_i).

Given a stable population of sexually reproducing pairs, I combine $l_m R = 2$ from eqn 9, with eqns 4 and 15 to estimate net energy as

$$\epsilon = \frac{2w_\epsilon(w_j + t_e\beta\bar{w}_j)}{l_m\, t_r\, w} \tag{16}$$

and resource handling as $\alpha = \epsilon W/\beta$.

Following Witting (2017a), the gross energy of a pure replicating individual—that does not participate in interactive competition and allocates all its net energy into replication—is net energy plus total metabolism. Yet, especially males use net energy in interactive competition, with the predicted fraction of the total net energy (ϵn_r) that is used in interactive competition being $1-\theta$ for replicating units with n_r individuals where $\theta = 1/n_r$.

Assuming that interactive energy is burned by extra metabolism, we find on average that the total metabolism of an organism

$$w\beta = w\beta_g + w\beta_n \tag{17}$$

contains a partial net component

$$w\beta_n = (1-\theta)\epsilon \tag{18}$$

that reflects the net energy that is burned in interactive competition, and a partial gross component β_g that defines the difference between gross and net energy, thus

$$\epsilon_g = \epsilon + w\beta_g = \epsilon + w\beta - w\beta_n \tag{19}$$

$$= \quad \theta\epsilon + w\beta$$

with $\theta = 0.5$ for populations of sexually reproducing pairs.

C Estimation sequence

To estimate life history traits for all species with body mass estimates, I used a sequence of calculation where data and missing parameter estimates are constrained by the underlying demography, growth and energetic. This estimation includes four filters (see filter SI) that use model constraints and data distributions to adjust unexpected estimates for lifespan, adult survival, gross energy, and the growth rated parameters $\acute{w}_0$, $\acute{w}_j$ and t_j.

I converted data on brood size (m_b), brood frequency (m_f) and/or brood interval (m_i) to yearly reproduction ($m = m_b m_f$, $m_f = 1/m_i$); and data on sexual maturity (t_s) to reproductive maturity ($t_m = t_s + t_p$). Data on total metabolism (βw) were transformed to metabolic rates per unit mass (β), and the ratio ($\beta/\underline{\beta}$) of field (β) over basal ($\underline{\beta}$) metabolism was calculated for all species with data on both. Mortality ($q_{ad} = 1 - p_{ad}$) data were calculated from survival rates (p_{ad}) to have two mirror estimates of all survival data.

Missing values were then estimated for m, t_p, t_j, t_m, t_l, $\acute{w}_0$, $\acute{w}_j$, h, N, $\underline{\beta}$, $\beta/\underline{\beta}$, p_{ad} and q_{ad}. Missing values for field metabolism (β) were obtained from the $\beta/\underline{\beta}$-ratio and basal metabolism. Missing values for p_{ad} and q_{ad} were first estimated independently by allometric correlations on p_{ad} and q_{ad}, and adjusted afterwards to identical mirror values in order to avoid unrealistic estimates where $p_{ad} > 1 \wedge q_{ad} < 0$ or $p_{ad} < 0 \wedge q_{ad} > 1$. With $\bar{p_{ad}}$ being the average survival rate for the two missing parameter estimates of p_{ad} and q_{ad}, the adjustment was done by setting $q_{ad} = 1 - p_{ad}$ for $\bar{p_{ad}} \leq 0.25$, by setting $p_{ad} = 1 - q_{ad}$ for $\bar{p_{ad}} \geq 0.75$, and by setting $p_{ad} = \bar{p_{ad}}$ and $q_{ad} = 1 - \bar{p_{ad}}$ for $0.25 < \bar{p_{ad}} < 0.75$.

A survival/mortality filter was constructed from an invariant $\acute{l}_m = l_m/p_{ad}^{t_m}$-ratio. As adult survival is larger than offspring and juvenile survival in most species, we expect the $\acute{l}_m$ ratio to be somewhat smaller than unity in nearly all species. From the $\acute{l}_m$ distributions across all species, I determined an upper limit on $\acute{l}_m$ of 0.8 for birds and 0.95 mammals. Then, as $l_m = 2/t_r m = 2(1 - p_{ad})/m$, we find that models with $\acute{l}_m$ ratios above these limits may have an estimate of the reproductive rate (m) that is too low, or an estimate of the reproductive age (t_m) that is too high, or an estimate of adult survival (p_{ad}) that is too low.

For species that failed to pass the survival filter (i.e., $\acute{l}_m > 0.8$ for birds; $\acute{l}_m > 0.95$ for mammals), I would fist examine for the possibility of outlier data for m and t_m. For this I would, for species with m and/or t_m data, estimate the corresponding missing parameter values for m and t_m. If one of the latter two estimates made the species pass the survival filter, I would classify the data value as an outlier. If no outlier was identified I would increase adult survival to obtain a $\acute{l}_m$ ratio that resembled the missing parameter estimate of $\acute{l}_m$ for that species. I would then remove the p_{ad} and q_{ad} outliers from the main data and rerun the complete estimation sequence until no extra outliers were identified.

Estimates were then calculated as $t_r = 1/(1 - p_{ad})$ by eqn 11, $t_g = t_m + p_{ad}/(1 - p_{ad})$ by eqn 12, $R = t_r m$, $l_r = p_{ad}^{t_r}$, and $l_m = 2/t_r m$ from zero growth $\lambda = l_m t_r m/2 = 1$ at equilibrium.

A lifespan filter adjusted unlikely small t_l values, and all growth related parameters $\acute{w}_0$, $\acute{w}_j$, and t_j were filtered for unexpected values, where after the parameters of eqn 1 were calculated as $\gamma_a = \ln(\ln[\acute{w}_0/\acute{w}]/\ln[\acute{w}_j/\acute{w}])/(t_j - t_0)$ and $\gamma_b = -e^{ct_j}\ln(\acute{w}_j/\acute{w})$. $\bar{w}_j$ was then estimated by eqn 5, net energy by eqn 16, gross energy by eqn 19 and the gross energy filter, resource handling as $\alpha = \epsilon/\beta$, home range overlap as $h_o = hN$, encounter rate as $v = \underline{\beta} w^{1/2d}/h^{1/d}$, and the level of interference as $I = h_o v$ followed by a rescaling to set $\iota = \ln I$ equal to unity at the median across all birds.

D Population dynamics

The age-structured population dynamic model is parameterised from the age of reproductive maturity in years (t_m), annual reproduction (m), and annual survival (p_{ad}) of adults. These parameters are converted to an appropriate timescale where the timestep of the iteration is $\Delta t \leq \min(1, t_m)$, with parameters scaled as $a_m = t_m/\Delta t$, $m^* = m\Delta t$, and $p = {p_{ad}}^{1/\Delta t}$.

The survival parameter p is used as the survival rate for all age-classes except age-class zero. To calculate age-class zero survival, I converted p into the reproductive period $t_r = 1/(1 - p)$, to calculate lifetime reproduction $R = t_r m^*$, and $l_m = 2/R$ from the equilibrium constraint $l_m R/2 = 1$. Age class zero survival is then calculated as $p_0 = l_m p^{1-a_m}$.

With $x \gg a_m$ being the maximum lumped age-class, the number $n_{a,t}$ of individuals of age $0 < a < x$ at timestep t is

$$n_{a,t} = p_{a-1} n_{a-1,t-1} \tag{20}$$

and the number in age-class x

$$n_{x,t} = p_x n_{x,t-1} + p_{x-1} n_{x-1,t-1} \tag{21}$$

with $p_a = p_0$ for $a = 0$ and $p_a = p$ for $a \geq 1$. Let the number of individuals in each age-class relate to time just after each timestep transition, with offspring at t being produced by the $t-1$ individuals that survive to the $t-1 \rightarrow t$ transition, with the density dependent ecology being approximated by the average 1+ abundance of the two timesteps:

$$\hat{n}_t = 0.5 \sum_{a \geq 1} n_{a,t} + n_{a,t-1} \tag{22}$$

The number of offspring in age-class zero is then

$$n_{0,t} = 0.5\ m^* \left(\frac{\hat{n}^*}{\hat{n}_t} \right)^{\gamma} \sum_{a \geq a_m} \tilde{m}_{a,t}\ n_{a,t} \tag{23}$$

where γ is the strength of density regulation, and $\tilde{m}_{a,t} = 1/q_{a,t}$, with $q_{a,t}$ being the average competitive quality of cohort a at t. At the population dynamic equilibrium $q_a^* = 1$ for all ages. More generally $q_{a,t} = q_{a-1,t-1}$ and

$$q_{x,t} = \frac{q_{x,t-1} p_x n_{x,t-1} + q_{x-1,t-1} p_{x-1} n_{x-1,t-1}}{n_{x,t}} \tag{24}$$

assuming that there is no change in the quality of a cohort over time. The quality of offspring

$$q_{0,t} = \frac{\sum_{a \geq a_m} q_{a,t}\ n_{a,t}}{\sum_{a \geq a_m} n_{a,t}} \left(\frac{\hat{n}_t}{\hat{n}^*} \right)^{\gamma_\iota} \tag{25}$$

is the average quality of the mature component multiplied by the density dependent selection, with γ_ι being the selection response.

For the initial conditions of an iteration I use the same quality across all individuals, and an initial abundance with a stable age-structure

$$c_a = l_a / \sum_{a \geq 0} l_a \tag{26}$$

where $l_0 = 1$, $l_a = p_0\ p^{a-1}$ for $1 \leq a < x$, and $l_x = p_0\ p^{x-1}/(1-p)$.